Acta Geotechnica (2020) 15:2649–2664
https://doi.org/10.1007/s11440-020-00933-9

RESEARCH PAPER

Effect of open-framework gravel on suffusion in sandy gravel alluvium

Yulong Luo[1] · Yi Huang[1]

Received: 14 January 2019 / Accepted: 2 February 2020 / Published online: 20 February 2020

Abstract
Some accidents of dams are attributed to suffusion around open-framework gravel (OFG) in sandy gravel alluvium. However, whether OFG can be really an internal seepage exit of fine particle migration in the field or not? How much the effect of OFG on suffusion is? These problems have not been investigated yet. This paper presented a list of flume-scale suffusion tests to investigate suffusion at the tip of a cutoff wall in sandy gravel alluvium with OFG. The results indicate that suffusion first initiates at the downstream side of the tip of the cutoff wall in the test without OFG, while in the tests with OFG, it initiates at the upstream side of OFG, and then both mainly progress backward to the upstream side. OFG significantly decreases the hydraulic gradients at the initiation of suffusion and at blowout. In addition, the experimental results also confirm that OFG is likely to be an internal seepage exit of fine particle migration in the field. A large number of fine particles and some coarse particles in the sandy gravel are eroded into OFGs in the tests, and OFG significantly increases the settlement induced by blowout; meanwhile, it makes the settlement unstable after blowout.

Keywords Internally unstable · Open-framework gravel · Sandy gravel alluvium · Suffusion

1 Introduction

Suffusion is a phenomenon that involves the migration of fine particle in a coarser soil matrix and may induce unacceptable deformation [3, 9]. The unacceptable deformation induced by suffusion may damage main measures controlling the underseepage of dams, and eventually threat dam safety. Sandy gravel alluvium is the Quaternary unconsolidated sediment that has been accumulated in valleys. It has loose structure, lithologic discontinuity, complicated genetic types, non-uniform physical and mechanical properties, and high permeability. Sandy gravel alluvium always contains internally unstable soils and is prone to suffusion. In the worst-case scenario, sandy gravel alluvium also contains open-framework gravel (OFG) [11, 14, 19, 20, 26], OFG is always found in gravelly fluvial deposits, it occurs as planar strata and cross strata of varying scale, and it is interstratified with sand, sandy gravel, and gravelly sands [19, 20]. OFG is poorly graded gravel and classified as GP based on unified soil classification system (USCS) [14], and it has negligible sand content and large permeability. The large permeability is due to the lack of sediment blocking pore space between gravel grains. Based on the description of Lunt and Bridge [19], the permeability of OFG is one or two orders of magnitude greater than sandy gravel, and up to four orders of magnitude greater than sand [19].

Dams built on such sandy gravel alluvium containing internally unstable soils and OFG may be more susceptible to suffusion or seepage failure. On the one hand, OFG strata may be connected to form preferential flow pathways [11, 20], and it can provide enough space for the fine particles eroded from surrounding internally unstable sandy gravel. Consequently, OFG may decrease the hydraulic condition at the initiation of suffusion. Foster et al. [12] concluded that OFG was one of the most important factors influencing the initiation of suffusion. On the other hand, a large number of fine particles are eroded into OFG in the evolution of suffusion, and then, it may induce unacceptable deformation of foundation and eventually damage anti-seepage measures of dams. In the first impoundment of Tarbela Dam in Pakistan, the unacceptable deformation

✉ Yulong Luo
lyl8766@hhu.edu.cn

Yi Huang
seepagehhu@126.com

[1] College of Water Conservancy and Hydropower Engineering, Hohai University, Nanjing 210098, China

induced by suffusion was observed in the upstream impervious blanket, which is the main measure controlling the underseepage of the dam. Three hundred and sixty-two sinkholes and 140 cracks were found on the blanket. Most of the sinkholes have diameters in the range of 0.3–4.5 m and depths from about 1.2 to 1.8 m. The largest sinkhole is 12.2 m in diameter and 4.0 m in depth [31]. Ul Haq [31] and Fell et al. [10] inferred that the serious accident of Tarbela Dam was mainly attributed to suffusion around OFGs in the deep sandy gravel alluvium foundation. In addition, the accidents of Three Sisters Dam in Canada and Mogoto Dam in South Africa are also induced by suffusion around OFGs [12].

At present, cutoff walls have been widely used to control underseepage of dams constructed on sandy gravel alluvium foundations [27]. The 30 case histories of dams assembled by Rice and Duncan [27] indicate that cutoff walls drastically increase hydraulic gradients around the boundaries of the walls and significantly give rise to suffusion. Under extreme adverse conditions in the field, if OFG is adjacent to the tip of a cutoff wall, as depicted in Fig. 1, suffusion around the tip of cutoff wall and OFG may be a significant threat for dam safety. However, how much the effect of OFG on suffusion is? Whether OFG can be an internal seepage exit of fine particle migration in the field or not? These problems have not been investigated yet. So it is worthy of investigating these two problems.

For suffusion to occur, two criteria have to be satisfied: (a) a geometric criterion: Several geometric criteria have been proposed to evaluate internal instability of soils, such as Kenney and Lau [15], Wan and Fell [33], Li and Fannin [17], Indraratna et al. [13], Chang and Zhang [6], and Marot et al. [23]; and (b) a hydromechanical criterion: Suffusion is always governed by hydraulic gradient and effective stress within soils [5, 18, 21, 22]. The topic of this study is related to the hydraulic criterion of suffusion. At first, effect of hydraulic gradient on suffusion was investigated. The tests performed by Skempton and Borgan [29] found that the critical hydraulic gradient initiating suffusion in internally unstable sandy gravel was far lower than that given by Terzaghi [30]. Recently, effect of stress state on suffusion was also considered. Bendahmane et al. [4] underlined the effect of confining pressure on suffusion. Moffat et al. [24] investigated the spatial and temporal progressions of suffusion under uniaxial load. Moffat and Fannin [25] found that the critical hydraulic gradient at the initiation of suffusion increased with the increase in mean vertical effective stress. Chang and Zhang [5] investigated the effects of confining pressure and deviator stress on suffusion, and they defined three critical gradients termed as initiation, skeleton deformation, and failure hydraulic gradients. Luo et al. [21] investigated the effect of deviator stress on the initiation of suffusion. The results indicate that deviator stress has significant influence on the initiation of suffusion. Based on the experimental results, an empirical method determining the critical hydraulic gradients under complex stress states was also developed. Luo et al. [22] focused on suffusion at the bottom of a cutoff wall in an internally unstable sandy gravel alluvium. The results suggested that the hydraulic gradients at the initiation of suffusion and at blowout linearly increased with the increase in overburden pressure. However, only a single layer of sandy gravel alluvium was considered by Luo et al. [22]. In addition, Correia dos Santos et al. [7, 8] investigated the crack-filling ability of gap-graded sandy gravels, which are susceptible to suffusion and are located upstream of an erosion path in the core of a zoned dam. The experimental results indicate that the sand content of the sandy gravel, and its relation with D_{15F} of the downstream filter, is critical for rapid crack filling to occur.

It can be seen that present studies mainly focus on the suffusion geometric and hydromechanical criteria of internally unstable soils; however, the influence of OFG on the evolution of suffusion, which is the main reason inducing serious accidents of dams [10, 12, 31], has not been investigated yet. The objective of this study focused on this influence. Two soils, internally unstable sandy gravel and internally stable OFG, were tested, and the flume-scale suffusion apparatus designed by Luo et al. [22] was employed. First, as a benchmark, one flume-scale suffusion test without OFG was performed to investigate the evolution of suffusion in sandy gravel alluvium.

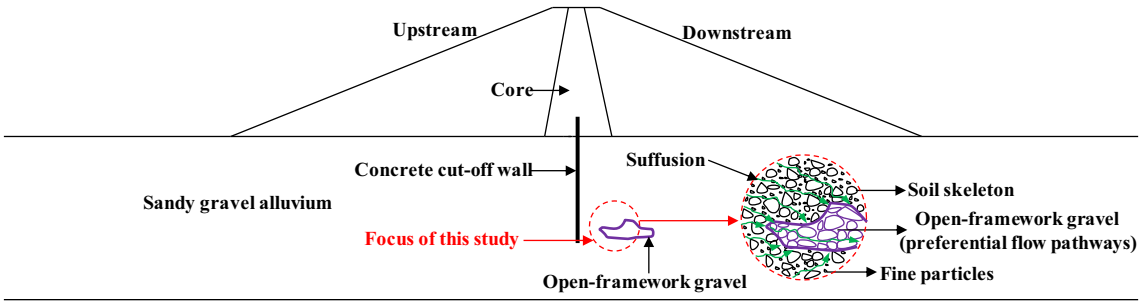

Fig. 1 Illustration of suffusion around OFG and the tip of a cutoff wall in sandy gravel alluvium

Second, four flume-scale suffusion tests with sandy gravel and OFG were then carried out to investigate the effect of OFG on suffusion. Finally, effects of OFG on the settlement and fine particle migration were also studied comprehensively.

2 Methodology

2.1 Flume-scale hydromechanical suffusion apparatus

A flume-scale hydromechanical suffusion apparatus depicted in Fig. 2 was developed by Luo et al. [22]. The apparatus consists of an axial loading system, a seepage pressure system, a funnel-shaped drainage system, specimen container, and a data acquisition system. The axial loading system simulates the overburden pressure acting on soils, such as from a high earthen or rockfill dam, and it can provide a maximum pressure of 3.3 MPa. The seepage pressure system provides the driving power for fine particle migration, and it has two modes applying hydraulic head: a high mode (3 m $< h <$ 50 m) and a low mode ($h <$ 3 m). The high mode is realized by a pressurized water source, and the low mode is controlled by raising a water tank. The funnel-shaped drainage system is comprised of a downstream perforated plate with 5-mm pore opening size, a downstream catchment basin, and a funnel-shaped outlet. The eroded particles can pass through the downstream perforated plate into the funnel-shaped outlet freely and are collected in the downstream catchment basin. Pore opening size of the downstream perforated plate may have significant influence on suffusion. In previous studies [5, 16, 24], the ratio of pore opening size to the largest fine particle size ranges from 6.7 to 28.5; in this study, the ratio is 7.1, so it can be concluded that the adopted pore opening size is suitable. The specimen container is used to compact a specimen with a cutoff wall. The data acquisition system consists of a vertical displacement transducer with a resolution of 0.01 mm to measure specimen deformation during test, a pressure transducer to record overburden pressure, and 22 pore pressure measurements in the specimen. Pore pressure probe and plastic tube with an external diameter of 4 mm are installed in specimen and connected

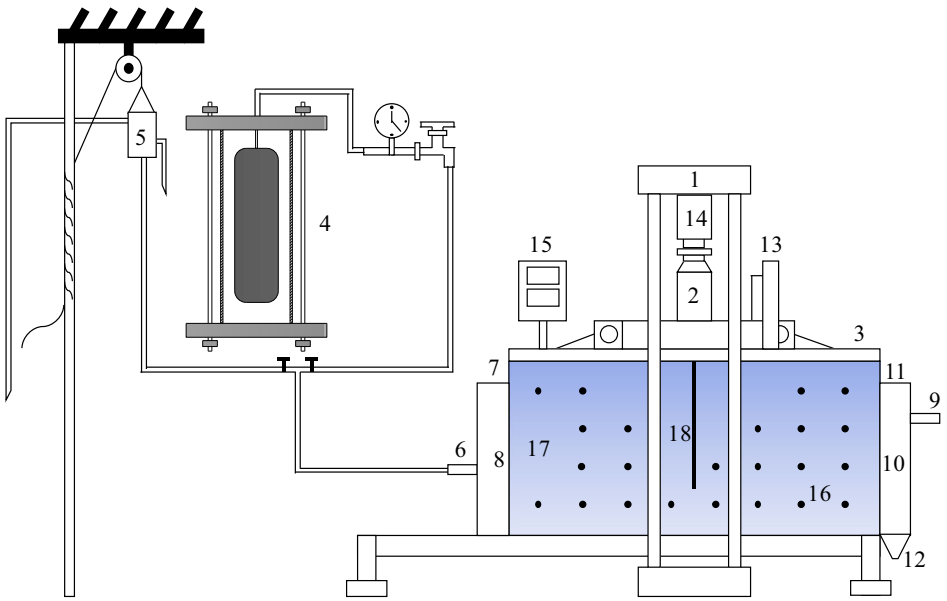

Axial loading system:
1 Reaction frame; 2 Jack; 3 Steel loading plate
Seepage pressure system:
4 Pressurized water source(for 3 m <h< 50 m); 5 Constant-head water tank (for h< 3 m); 6 Inlet pipe
7 Upstream catchment basin; 8 Upstream porous plate (5mm pore opening size); 9 Outlet pipe
Funnel-shaped drainage system:
10 Downstream porous plate (5mm pore opening size); 11 Downstream catchment basin; 12 Funnel-shaped outlet
Data acquisition system:
13 Vertical displacement transducer; 14 Axial pressure transducer; 15 Displacement and pressure displayer
16 Pore pressure measurement
Specimen container:
17 Specimen; 18 Cutoff wall

Fig. 2 Sketch of the flume-scale hydromechanical suffusion apparatus [22]

to the pore pressure transducer located outside of the specimen. In order to reduce the impact of plastic tube on the erosion process, the plastic tubes used in this study are as small as possible. Meanwhile, all the pore pressure measurements were installed on the central axis of specimen to eliminate boundary effect. The following experimental results also indicate that the impact of plastic tube on erosion process is small.

2.2 Characteristics of the testing soils

Figure 3 depicts the particle size distributions of the two testing soils. Sandy gravel is similar to that in Luo et al. [22], and the main difference is the largest particle size. The largest particle sizes of the sandy gravels in this study and Luo et al.'s [22] are 40 mm and 60 mm, respectively. Decreasing the largest particle size can improve the reliability of test results. Based on the study of Lunt et al. [20], the particle size distribution of OFG is significantly different from that of surrounding sand or sandy gravel. Consequently, in order to represent the main characteristics of OFG in the field, the OFG in this study is similar to that reported by Lunt et al. [20], as depicted in Fig. 3. It is composed of gravels with diameters ranging from 2 to 40 mm. Table 1 depicts the assessment of internal stability of the two soils using several geometric criteria [6, 15, 17, 33]. According to the geometric criteria, the sandy gravel is internally unstable, whereas the OFG is internally stable. Base on the method proposed by Wan and Fell [32], the largest fine particle size for the sandy gravel is 0.7 mm, and corresponding fine particle content is about 19%, which is lower than the critical value (29% for loose state or 24% for dense state) postulated by Kenney and Lau [15]. So this sandy gravel has large internal voids that fine particles can enter. According to ASTM D2434-68 [1], the permeability of the sandy gravel and OFG is approximately 2.3×10^{-2} cm/s and 2.21 cm/s, respectively. The permeability of the OFG is also consistent with that reported in Lunt et al. [20].

2.3 Specimen preparation and instrumentation

Table 2 shows the summary of the five suffusion tests. As a benchmark, one suffusion test without OFG, which is termed as test N-OFG, was performed first. Figure 4a shows the schematic of specimen and instrumentation configuration of test N-OFG. The specimen is 1000 mm long, 500 mm high, and 300 mm thick. A flow condition around the cutoff wall in the field was simulated in this test. The cutoff wall was simulated by a steel plate that is 10 mm thick, 300 mm long, and 400 mm deep. A clay layer was placed along the upstream and downstream sidewalls, respectively, to create impermeable barriers, so that seepage flowed over the top of the upstream clay barrier, passed under the cutoff wall, and exited over the top of the downstream clay barrier. The clay barriers are 300 mm long, 340 mm high, and 50 mm thick. Sandy gravel is compacted at a water content of 5% and a dry density of 2.36 g/cm^3, and the relative density is approximately 80%. Geotextiles were placed at the interfaces between the clay layers and sandy gravel to prevent contact erosion. After the compacted soil specimen reached the bottom elevation of the cutoff wall, the cutoff wall was slid into the specimen container along two rubber-lined grooves on the

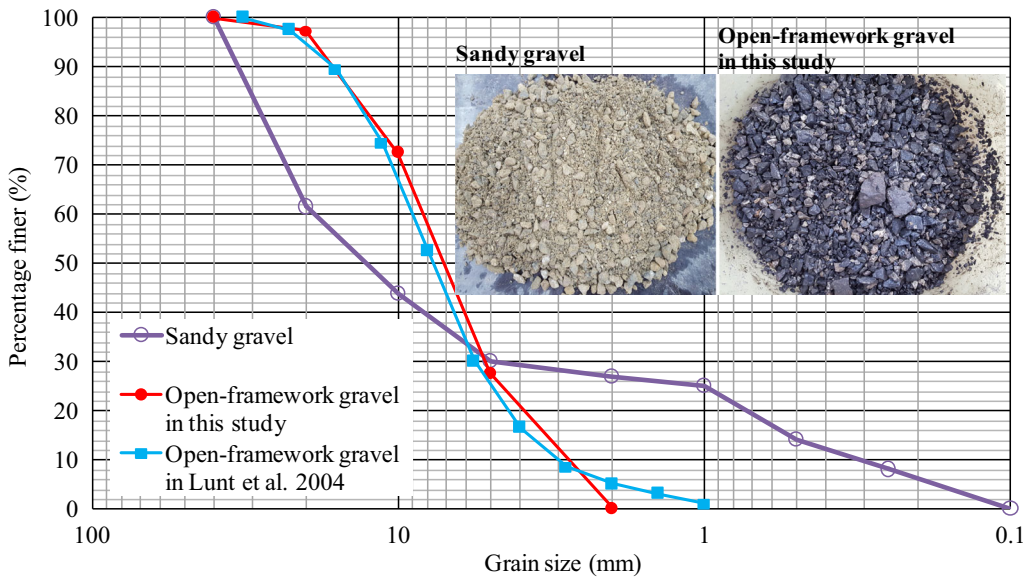

Fig. 3 Particle size distributions of the testing soils

Table 1 Evaluation of internal instability of the testing soils

Criteria	Material description	The soil is internally stable if	Internally unstable	
			Sandy gravel	OFG
Kenney and Lau [15]	Granular soils	$(H/F)_{min} > 1$, For broadly graded soil, $0 < F < 20\%$; For narrowly graded soil, $0 < F < 30\%$	Y	N
Wan and Fell [33]	Broadly graded and gap-graded soils	$P = e^Z/[1 + e^Z]$ $Z = 3.875\log(h'') - 3.591\ h' + 2.436$ for sand–gravel mixtures	Y	N
Li and Fannin [17]	Granular soils	For $F < 15\%$, $(H/F)_{min} \geq 1.0$; For $F > 15\%$, $H \geq 15\%$	Y	N
Chang and Zhang [6]	Broadly graded soils	$P' < 5$, $(H/F)_{min} > 1.0$; $5 \leq P' \leq 20$, $(H/F)_{min} > -(1/15)P' + 4/3$; $P' > 20$, stable	Y	N

F = mass fraction at any grain size d; H = mass fraction between grain size d and $4d$; P = probability of internal instability; $h' = d_{90}/d_{60}$; $h'' = d_{90}/d_{15}$; d_{90}, d_{60}, and d_{15} = diameters of 90%, 60%, and 15% mass passing, respectively; P' = fine particle content (< 0.063 mm) defined by Chang and Zhang [6]; Y = internally unstable; N = internally stable

sidewalls in order to minimize sidewall leakage. Compaction of the soil continued with the cutoff wall in place until the top of specimen reached the top of the cutoff wall. Care was taken to ensure the same compaction around the cutoff wall as in the rest of the specimen. Survey points C1–C22 in Fig. 4a denote the 22 pore pressure measurements installed in the specimen. Based on previous study [22], suffusion at the tip of the cutoff wall can be detected by the variation of measured pore pressures at the tip of the cutoff wall, so the survey points installed at the tip of cutoff wall are denser than the rest of specimen. In addition, overburden pressure also has significant effect on suffusion [22], so an overburden pressure of 0.2 MPa was applied in this study. The applied pressure in this study is used to simulate the overburden pressure caused by an earthen dam in a sandy gravel alluvium in the field. Luo et al. [22] mainly investigated the influence of vertical pressure on suffusion in single-layered sandy gravel alluvium. Therefore, the influence of vertical pressure on suffusion was not studied here, and this study mainly investigated the influence of OFG on suffusion in a sandy gravel alluvium.

Table 2 Summary of the suffusion tests in this study

Test no.	Testing soil	Overburden pressure (MPa)	Coordinate of the centroid of OFG (x_c, y_c) (cm)
N-OFG	Sandy gravel	0.2	Without OFG
OFG-H1	Sandy gravel and OFG	0.2	(10.5, 0)
OFG-H2			(15.5, 0)
OFG-H3			(20.5, 0)
OFG-H4			(25.5, 0)

x_c is the horizontal coordinate of OFG centroid (cm); y_c is the vertical coordinate of OFG centroid (cm)

Another four suffusion tests with OFG and sandy gravel were carried out to investigate the effect of OFG on suffusion in sandy gravel alluvium. In each test, the OFG, which is 80 mm long, 80 mm high, and 300 mm thick, was installed at the downstream side of the tip of the cutoff wall, because based on the study of Luo et al. [22] suffusion first initiates at the downstream side of the cutoff wall. Meanwhile, Jussel et al. [14] and Lunt and Bridge [19] report that OFG is commonly in the order of centimeters to decimeters thick, meters to tens of meters in lateral extent in the field. The horizontal coordinate of the centroid of OFG varies from 10.5 to 25.5 cm. Figure 4b shows the schematic of specimen and instrumentation configuration of test OFG-H1. In order to monitor the variation of pore pressure in the OFG during the whole process of suffusion test, two pore pressure measurements were specially installed at the upstream and downstream sides of the OFG, respectively, for example C21 and C22 in test OFG-H1. OFG is also compacted at a water content of 5% and a dry density of 2.36 g/cm^3, and the relative density is approximately 73%.

2.4 Experimental procedures

After specimen preparation and instrumentation installation, specimen container was covered by a loading plate, and the top of the cutoff wall was connected into a rubber-lined groove in the loading plate. An inflated rubber tire encapsulated the perimeter of the loading plate and tightly fitted into the inner walls of the specimen container to prevent seepage leakage. A preferred overburden pressure

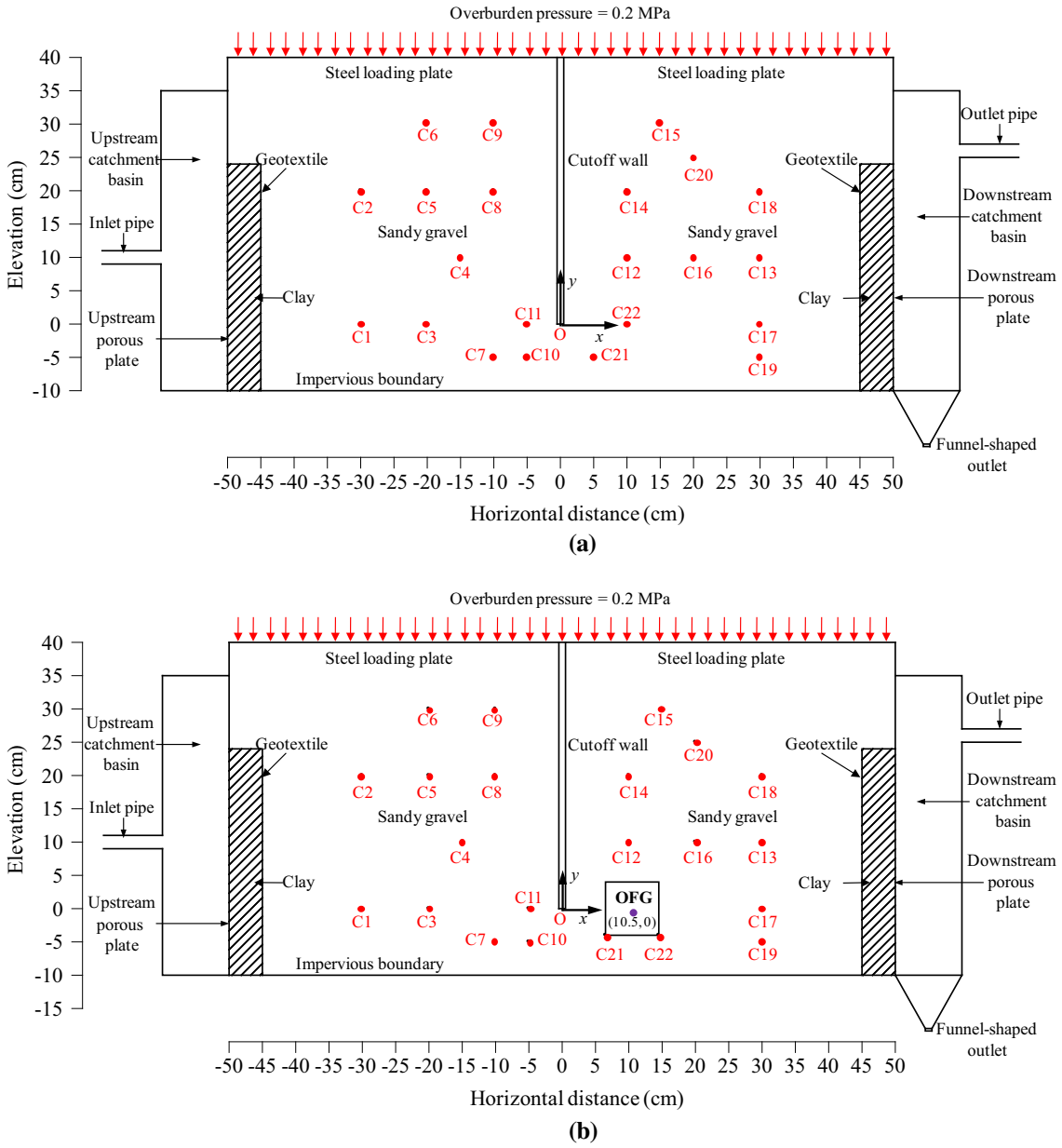

Fig. 4 Schematic of specimen and instrumentation configuration of suffusion tests (vertical section view): **a** test N-OFG and **b** test OFG-H1

of 0.2 MPa was gradually applied onto the loading plate, and then, saturation started. In general, the presence of air has profound implications on the results of suffusion test, so great efforts have been made to ensure the saturation of specimen in this study. In every test, saturation time was enough long; meanwhile, saturation started under a low hydraulic head difference. For example, in test OFG-H1, saturation started under a hydraulic head difference of 18.7 cm, and saturation time was approximately 4 h. Effluent was constantly monitored and no fine particle migration was observed during saturation. Pore pressure transducer and air escape valves on the top loading plate were turned on to expel air until no escaped air bubbles were observed. When inflow rate was equal to outflow rate, specimen was fully saturated. After saturation, seepage was introduced into the specimen under different step-increase hydraulic head differences. Under each step, flow rate and settlement were recorded in every 10-min interval. In the whole process of test, a high-definition camera was used to monitor the migration of fine particle through the transparent Plexiglas wall. In addition, the phenomena including fine particle migration and leakage channel evolution were also observed and recorded. If flow rate no longer changed and no further soil loss was observed, the pore pressures at

22 locations were recorded, and then, the next step of hydraulic head difference was applied. The range of total hydraulic head difference between the upstream and downstream sides (ΔH) applied was different in different tests. For example, in test N-OFG, there were nine steps in the whole process of the test and ΔH varied from 46.2 to 647.4 cm; in test OFG-H1, there were 11 steps and ΔH varied from 18.7 to 684.5 cm. Based on the study of Sibille et al. [28], the failure induced by suffusion was defined as "blowout," which was characterized by an increased particle migration within a short time period (blowout of fine particles) and produced rapid, large settlement of specimen. So, in this study blowout was also adopted. After each test, sieve analyses on the specimen and eroded particles collected by the funnel-shaped drainage system were performed according to ASTM D6913-04 [2].

3 Results and discussion

3.1 Evolution of suffusion in the test without OFG

Suffusion at the tip of the cutoff wall is a localized phenomenon, and capturing the initiation of suffusion and blowout is a great challenge. In this study, the method proposed by Luo et al. [22] was adopted to determine the initiation of suffusion and blowout. Measured pore pressures and derived hydraulic gradient at the tip of the cutoff wall, which are also localized parameters, are used as main indications of suffusion. With the increase in ΔH, a sudden change in pore pressure or hydraulic gradient at the bottom of the cutoff wall indicates the initiation of suffusion. Further increase in ΔH eventually induces blowout. Significant change in pore pressure or hydraulic gradient around the bottom of the cutoff wall is observed again. In addition, some secondary indications also have significant changes at blowout. For example, some coarse particles are observed to migrate at the bottom of the cutoff wall, flow rate starts to change nonlinearly, and effluent becomes turbid.

Figure 5a shows the variation of hydraulic gradient around the tip of the cutoff wall in test N-OFG. It should be noted that the values of hydraulic gradient in Fig. 5a are not the local hydraulic gradient calculated exactly on the same flow lines; rather, they show approximate variation of hydraulic gradient around the cutoff wall. The hydraulic gradient between C10 and C21 ($i_{10–21}$), which is the ratio of the hydraulic head difference between C10 and C21 to their distance, first increased linearly with the increase in ΔH, and then, it started to decrease from 3.43 at ΔH = 141.3 cm to 2.77 at ΔH = 177.1 cm. Similarly, $i_{21–22}$ started to decrease from 2.73 at ΔH = 141.3 cm to 2.40 at ΔH = 177.1 cm. In addition, at ΔH = 141.3 cm and at ΔH = 177.1 cm, slight migration of fine particle, which occurred in the pore space between gravel grains, was observed at the tip of the cutoff wall and at outlet. Simultaneously, flow rate started to vary nonlinearly and it increased from 57.14 ml/s at ΔH = 141.3 cm to 80.5 ml/s at ΔH = 177.1 cm, as depicted in Fig. 6. Effluent became turbid at ΔH = 177.1 cm. According to the main and secondary indications of suffusion mentioned above, it can be judged that suffusion initiated at ΔH = 141.3 cm. When ΔH increased to 285 cm, a significant decrease in hydraulic gradient at the tip of the cutoff wall was detected again, and the value of $i_{21–22}$ decreased from 2.40 at ΔH = 177.1 cm to 1.84 at ΔH = 285 cm. Meanwhile, $i_{7–10}$ and $i_{10–21}$ increased rapidly; for example, $i_{10–21}$ increased from 2.87 at ΔH = 177.1 cm to 3.75 at ΔH = 285 cm. In addition, an obvious concentrated leakage channel, which was not adjacent to any plastic tube, was observed at the downstream side of the cutoff wall, as depicted in Fig. 7, and a large number of fine particles and some coarse particles finer than 2 mm started to migrate in the channel, and effluent became significantly turbid. Based on the main and secondary indications of blowout, it can be judged that blowout occurred at ΔH = 285.0 cm.

In addition, as a comparison, Fig. 5b and c also depicts the variations of local water head at survey point and head drop at the tip of cutoff wall in the evolution of suffusion. In the two figures, h is the local water head at a survey point and Δh is the local water head drop between two survey points. For example, h_7 and h_{10} are the local water heads at the two survey points C7 and C10, respectively, $\Delta h_{7–10}$ is the local water head drop between C7 and C10, and $\Delta h_{7–10} = h_7 – h_{10}$. It can be seen from Fig. 5 that the variations of average hydraulic gradient, local water head, and head drop at the tip of the cutoff wall can indicate the initiation of suffusion and blowout in each test. Meanwhile, the variations of average hydraulic gradient and local water head drop have the similar variation trends; using them as the indicators of suffusion is easier than using the variation of local water head.

Figure 8 shows the evolution of average hydraulic gradient around the tip of the cutoff wall in test N-OFG. The legends "high," "medium," and "low" in Fig. 8 represent comparatively high, medium, and low gradients, respectively. It can be seen that Fig. 8 intuitively depicts the evolution of suffusion around the tip of the cutoff wall in sandy gravel alluvium without OFG. Suffusion first initiated at the downstream side of the tip of the cutoff wall, and then, it generally progressed backward to the upstream side. Before the initiation of suffusion, $i_{10–21}$ and $i_{21–22}$ are comparatively high around the cutoff wall, $i_{7–10}$ and $i_{22–16}$ are medium, and $i_{4–7}$ and $i_{16–18}$ are low. It indicates that the

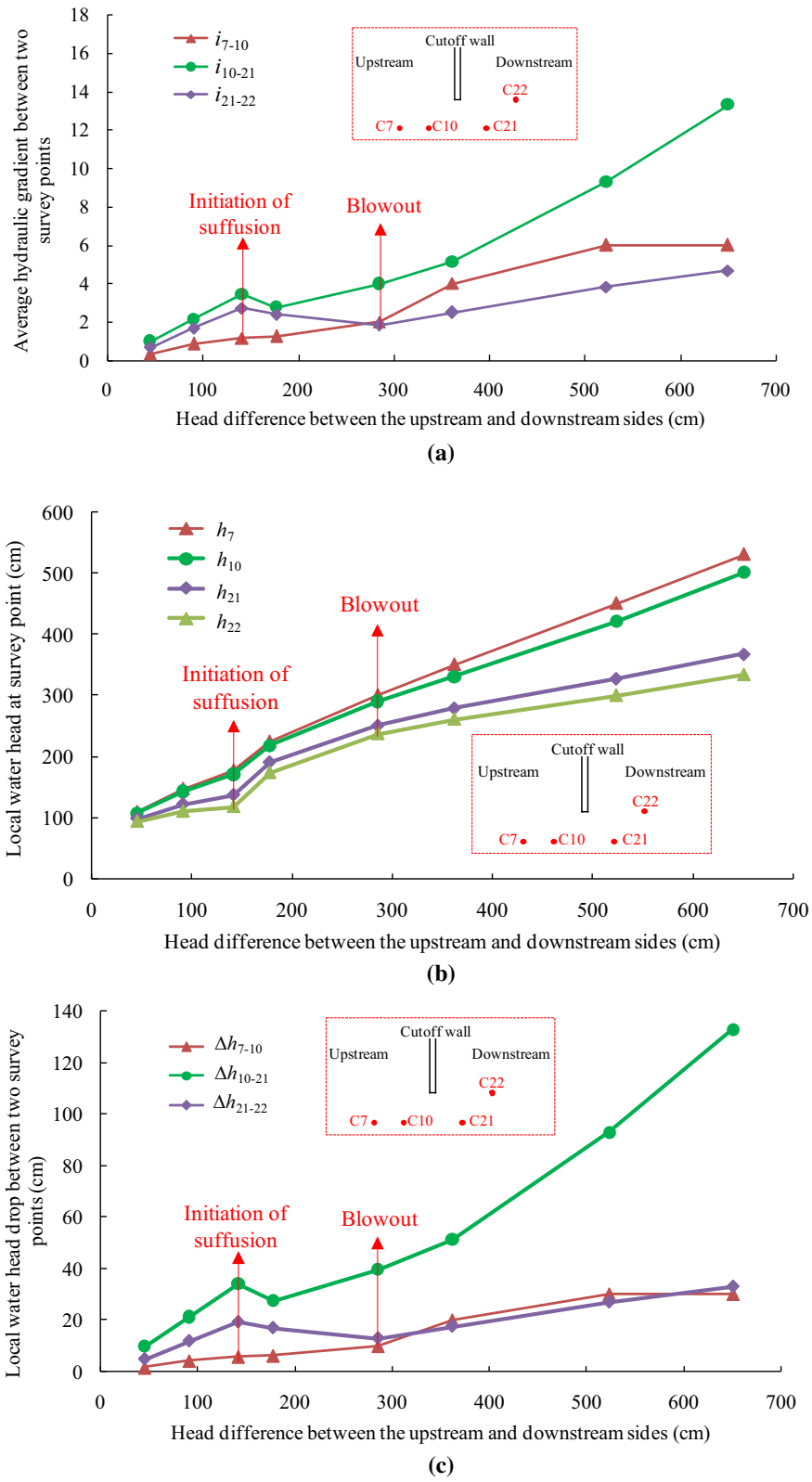

Fig. 5 Variations of hydraulic conditions at the tip of the cutoff wall (test N-OFG): **a** average hydraulic gradient; **b** local water head; and **c** local water head drop

tip of the cutoff wall (C10 and C21) and the downstream side of the tip (C21 and C22) mainly undertook ΔH before the initiation of suffusion. When ΔH increased to 141.3 cm, $i_{10–21}$ is still high, while $i_{21–22}$ becomes medium, and other gradients are comparatively low. It suggests that the permeability between C21 and C22 started to increase owing to the migration of fine particle, so suffusion first initiated at the downstream side of the tip of the cutoff wall (C21 and C22). When blowout appeared at ΔH = 285.0 cm, $i_{10–21}$ is still high, $i_{4–7}$, $i_{7–10}$, $i_{21–22}$, and $i_{16–18}$ become comparatively medium, and $i_{22–16}$ is low. It indicates that suffusion started to progress backward to the upstream side at this time. When ΔH increased to 522.5 cm, $i_{10–21}$ is still high, it is up to 9.3, $i_{4–7}$ and $i_{7–10}$ become comparatively medium, and $i_{21–22}$, $i_{22–16}$, and $i_{16–18}$ become low. It suggests that the upstream side (C4 and C7, and C7 and C10) and the tip of the cutoff wall (C21 and C22) mainly undertook ΔH after blowout, and the downstream side no

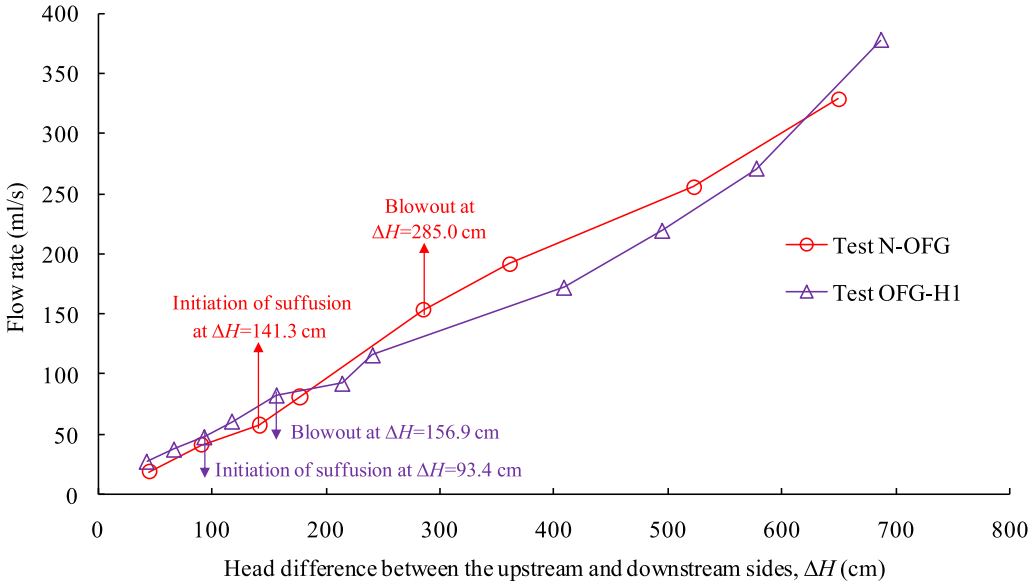

Fig. 6 Relationship between ΔH and flow rate in test N-OFG

Fig. 7 Downstream concentrated leakage channel after test N-OFG

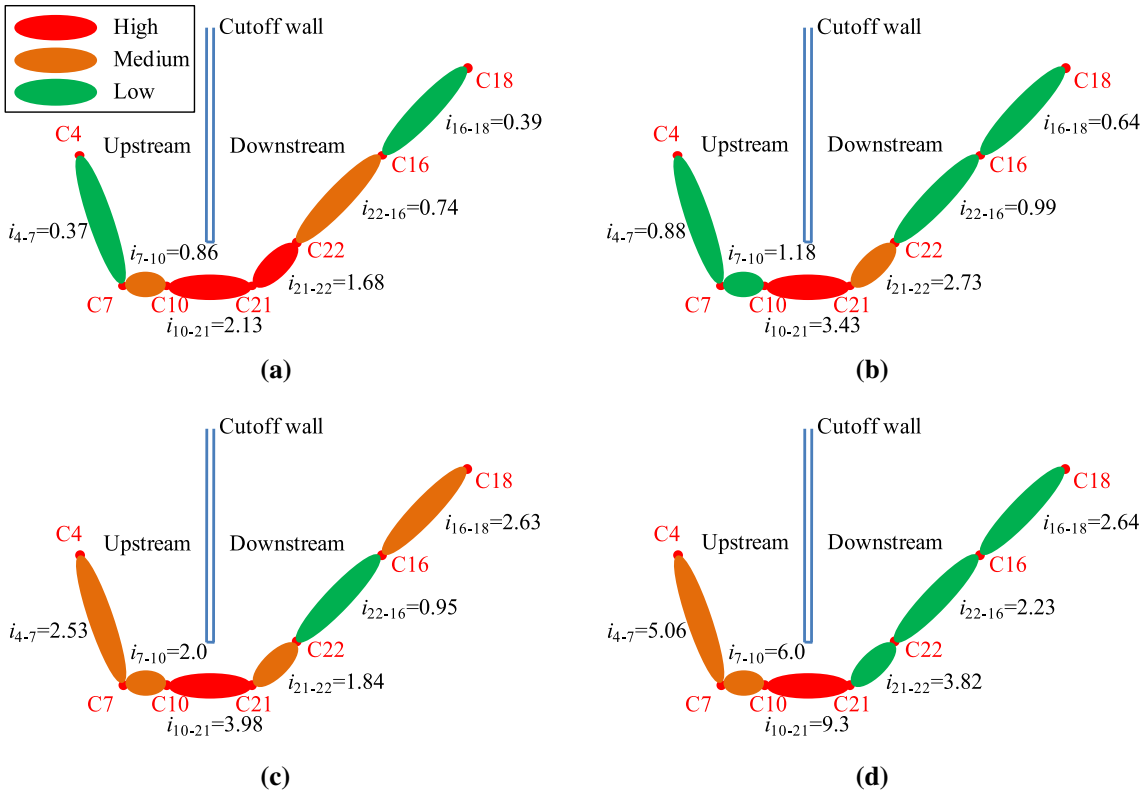

Fig. 8 Development of average hydraulic gradients around the tip of the cutoff wall in the evolution of suffusion (test N-OFG): **a** at ΔH = 90.9 cm, before the initiation of suffusion; **b** at ΔH = 141.3 cm, initiation of suffusion; **c** at ΔH = 285.0 cm, blowout; and **d** at ΔH = 522.5 cm, after blowout

longer undertook ΔH. Suffusion had completely progressed to the upstream side after blowout.

Comparisons between the results in test N-OFG and Luo et al. [22] may prove that the experimental program in this study is repeatable. Four flume-scale suffusion experiments in sandy gravel alluvium with a cutoff wall, which are similar to test N-OFG in this study, were conducted by Luo et al. [22] to investigate the influence of overburden pressure on suffusion. The sandy gravel used in Luo et al. [22] is also similar to that in this study, and the main difference is the largest particle size. The largest particle sizes of the sandy gravels in Luo et al.'s [22] and in this study are 60 mm and 40 mm, respectively. The experimental results indicated that the evolution of suffusion depicted in test N-OFG was significantly consistent with that revealed by Luo et al. [22].

Figure 9 shows the settlement in the evolution of suffusion in test N-OFG. The settlement at the beginning of the suffusion test is 2.06 mm, which was induced by the applied overburden pressure before the suffusion test. It can be seen that settlement first kept constant before the initiation of suffusion, and then, it suddenly increased to 2.08 mm at the later stage of ΔH = 177.1 cm, when blowout occurred at ΔH = 285.0 cm, it increased suddenly and significantly at the late stage of blowout, and it increased from 2.08 to 2.14 mm, and eventually it kept constant again after blowout. In addition, it should be clarified that the measured settlement in this study is not the localized settlement where blowout occurred, but it is an average settlement of the entire soil surface. So it can be inferred that the localized settlement induced by blowout in the field may be large enough to damage the measures controlling the underseepage of dams, such as concrete cutoff wall.

3.2 Evolution of suffusion in the tests with OFG

It is noted that only the experimental results of test OFG-H1 are described comprehensively in this section. Similar results and evolution trends also appeared in the other three tests with OFG. Figure 10 shows the variation of hydraulic gradient around the tip of the cutoff wall in test OFG-H1. When ΔH increased from 42.8 to 93.4 cm, the values of $i_{7–10}$ and $i_{10–21}$ increased linearly; simultaneously, $i_{21–22}$, which is the average hydraulic gradient of OFG, ranged from 0.01 to 0.06 owing to the high permeability of OFG. When ΔH increased from 93.4 to 117.7 cm, $i_{10–21}$ started to decrease from 1.06 at ΔH = 93.4 cm to 0.79 at ΔH =

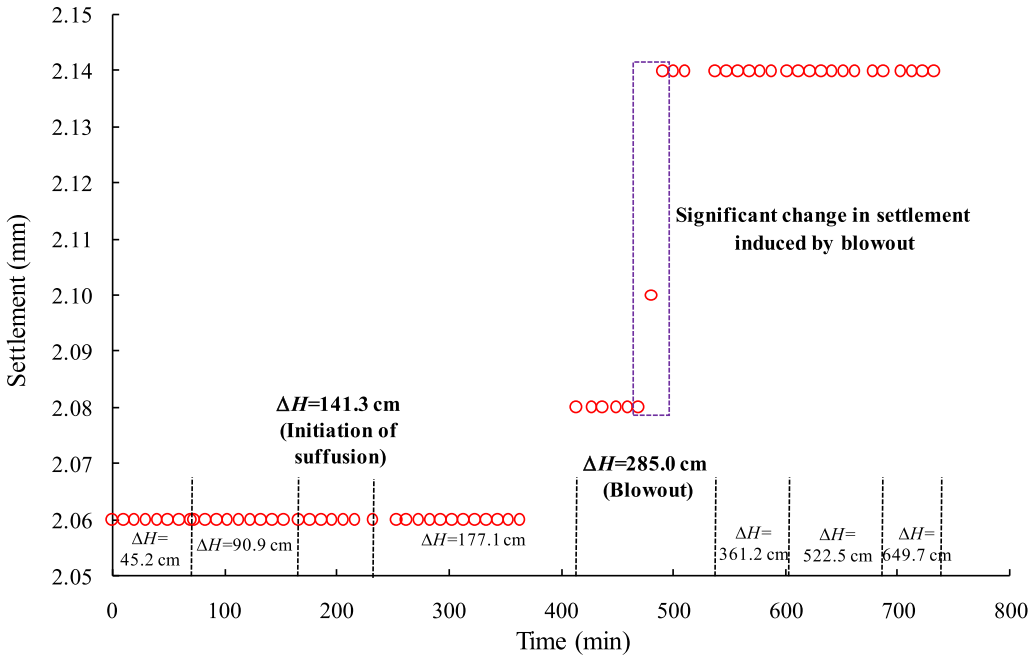

Fig. 9 Settlement in evolution of suffusion (test N-OFG)

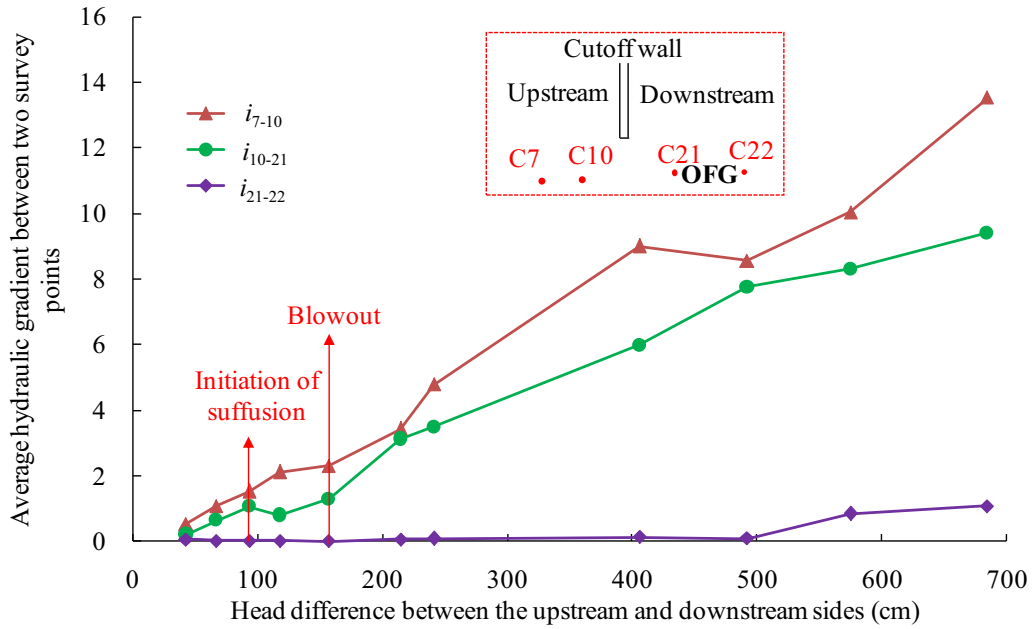

Fig. 10 Variation of average hydraulic gradient at the tip of the cutoff wall (test OFG-H1)

117.7 cm. The value of $i_{7–10}$ still increased linearly, and $i_{21–22}$ kept constant. In addition, at ΔH = 93.4 cm and ΔH = 117.7 cm, slight migration of fine particle was also observed at the tip of the cutoff wall. Meanwhile, effluent became turbid at ΔH = 93.4 cm. According to the main and secondary indications of suffusion, it can be judged that suffusion initiated at ΔH = 93.4 cm at the upstream side of the OFG (C10 and C21). When ΔH increased from 156.9 to 214.6 cm, the values of $i_{7–10}$ and $i_{10–21}$ no longer increased linearly; especially for $i_{10–21}$, it increased significantly from 1.28 at ΔH = 156.9 cm to 3.13 at ΔH = 214.6 cm. Meanwhile, an obvious concentrated leakage channel was observed at the tip of the cutoff wall at ΔH = 156.9 cm, and intensive migration of fine particle was also found in the channel, and flow rate started to increase nonlinearly, it increased from 82.4 ml/s at ΔH = 156.9 cm to 92.2 ml/s at ΔH = 214.6 cm, as depicted in Fig. 6, and effluent was significantly turbid. Based on the

main and secondary indications of blowout, it can be judged that blowout occurred at ΔH = 156.9 cm.

Compared with the results of test N-OFG, it can be found that OFG significantly decreases the hydraulic conditions at the initiation of suffusion and at blowout. In addition, it should be noted that the value of $i_{21–22}$ suddenly and significantly increased from 0.09 at ΔH = 492.2 cm to 0.84 at ΔH = 575.1 cm at the later stage of test OFG-H1. It indicates that a large number of fine particles were eroded into the OFG after blowout, so it can be inferred that OFG is likely to be an internal seepage exit of fine particle migration in the field.

Figure 11 shows the evolution of average hydraulic gradient around the tip of the cutoff wall in test OFG-H1. It can be seen that suffusion around the OFG and the tip of the cutoff wall, as depicted in Fig. 11, is significantly different from that without OFG, as shown in Fig. 8. Suffusion first initiated at the upstream side of the OFG, and then, it mainly progressed backward to the upstream side. Before the initiation of suffusion, as depicted in Fig. 11a, $i_{7–10}$ is comparatively high around the cutoff wall, and $i_{21–22}$ is low, and other gradients are medium. It indicates that the upstream side of the OFG (C7 and C10) mainly undertook ΔH before the initiation of suffusion. When ΔH increased to 93.4 cm, as depicted in Fig. 11b, $i_{7–10}$ and $i_{10–21}$ become comparatively high and $i_{21–22}$ is still low. It indicates that C10 and C21 did not have the ability to undertake ΔH; suffusion first initiated at the upstream side of the OFG (C10 and C21). When blowout appeared at ΔH = 156.9 cm, $i_{7–10}$ is still high, while $i_{10–21}$ becomes medium again. It indicates that suffusion started to progress backward to the upstream side. When ΔH increased to 575.1 cm, $i_{7–10}$ and $i_{10–21}$ become high, $i_{4–7}$ and $i_{16–18}$ become medium, and $i_{21–22}$ and $i_{22–16}$ are low. It indicates that the upstream side of the OFG mainly undertook ΔH, and the OFG and its downstream side no longer undertook ΔH. Suffusion had completely progressed to the upstream side of the OFG after blowout, as depicted in Fig. 11d.

3.3 Effect of horizontal position of OFG on suffusion

Table 3 and Fig. 12 show the hydraulic conditions at the initiation of suffusion and at blowout in different tests. In the table and figure, x_c is the horizontal coordinate of OFG centroid (cm); ΔH_{cr} and ΔH_b are the total head differences (cm) between the upstream and downstream sides at the initiation of suffusion and at blowout, respectively; i_{cr} and i_b are the average hydraulic gradients at the initiation of suffusion and at blowout, respectively, and they are the

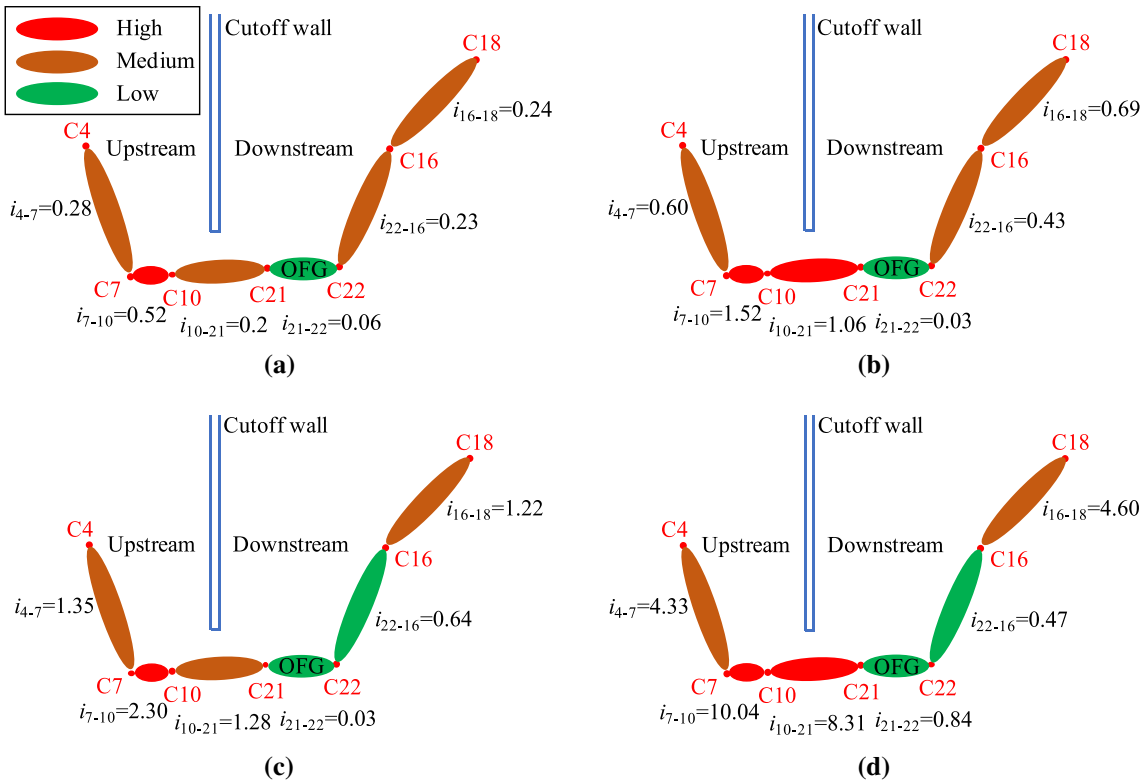

Fig. 11 Development of average hydraulic gradients around the tip of the cutoff wall in the evolution of suffusion (test OFG-H1): **a** at ΔH = 42.8 cm, before the initiation of suffusion; **b** at ΔH = 93.4 cm, initiation of suffusion; **c** at ΔH = 156.9 cm, blowout; and **d** at ΔH = 575.1 cm, after blowout

Table 3 Hydraulic conditions at the initiation of suffusion and at blowout in different tests

Test no.	x_c (cm)	x	ΔH_{cr} (cm)	i_{cr}	k_{cr}	ΔH_b (cm)	i_b	k_b
N-OFG	–	–	141.3	0.79	1.0	285.0	1.58	1.0
OFG-H1	10.5	0.058	93.4	0.52	0.66	156.9	0.87	0.55
OFG-H2	15.5	0.086	132.7	0.74	0.94	214.0	1.19	0.75
OFG-H3	20.5	0.114	134.0	0.74	0.95	207.6	1.15	0.73
OFG-H4	25.5	0.142	126.7	0.70	0.89	209.5	1.16	0.73

x_c is the horizontal coordinate of OFG centroid (cm); x is the characteristic distance of OFG, and it is the ratio of x_c to the seepage path length (180 cm) along the loading plate and cutoff wall; ΔH_{cr} and ΔH_b are the total head differences (cm) between the upstream and downstream sides at the initiation of suffusion and at blowout, respectively; i_{cr} and i_b are the average hydraulic gradients at the initiation of suffusion and at blowout, respectively, and they are the ratios of ΔH_{cr} and ΔH_b to the seepage path length (180 cm); k_{cr} and k_b are the reduction coefficients at the initiation of suffusion and at blowout, respectively, and they are the ratios of i_{cr} and i_b of tests with OFG to those of the test without OFG

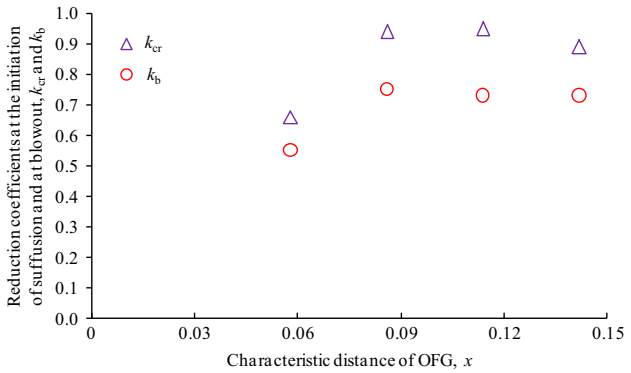

Fig. 12 Relationships between characteristic distance of OFG and reduction coefficients at the initiation of suffusion and at blowout

ratios of ΔH_{cr} and ΔH_b to the seepage path length (180 cm) along the loading plate and cutoff wall.

It should be noted that there are some abnormal experimental results in Table 3. For example, the value of ΔH_{cr} in test OFG-H4 is slightly less than those in tests OFG-H2 and OFG-H3 and that of ΔH_b in test OFG-H2 is slightly larger than those in tests OFG-H3 and OFG-H4. Actually, these abnormal results are acceptable. Because it is difficult to estimate and capture the critical hydraulic conditions of different tests, and in order to capture the critical hydraulic conditions, steps of applying hydraulic head difference were refined in each test. For example, in test OFG-H2, there were seven steps when ΔH ranged from 99.5 to 239.0 cm; in test OFG-H4, there were eight steps when ΔH ranged from 91.8 to 261.5 cm.

In order to establish dimensionless parameters to describe the influences of OFG on i_{cr} and i_b, three parameters, k_{cr}, k_b, and x, were proposed, as shown in Table 3, k_{cr} and k_b are the reduction coefficients at the initiation of suffusion and at blowout, respectively, and they are the ratios of i_{cr} and i_b of tests with OFG to those of the test without OFG. The values of k_{cr} and k_b reflect the effects of OFG on the initiation of suffusion and on blowout, respectively. x is the characteristic distance of OFG, and it is the ratio of x_c to the seepage path length (180 cm).

It can be seen from Table 3 and Fig. 12 that both OFG and the horizontal position of OFG have significant influences on the critical hydraulic conditions at the initiation of suffusion and at blowout. When x ranges from 0.058 to 0.086, the values of k_{cr} and k_b significantly increase with the increase in x, k_{cr} increases from 0.66 at $x = 0.058$ to 0.94 at $x = 0.086$, and k_b increases from 0.55 at $x = 0.058$ to 0.75 at $x = 0.086$. When x increases from 0.086 to 0.142, k_{cr} and k_b almost keep constant, k_{cr} ranges from 0.89 to 0.94, and k_b ranges from 0.73 to 0.75. Owing to the limited tests performed in this study and a lack of strict validation, empirical formulas describing the influences of OFG on suffusion were not fitted based on the above experimental results.

3.4 Effect of OFG on the settlement in the evolution of suffusion

It is noted that only the settlement of test OFG-H2 is described comprehensively in this section. Similar results and evolution trends also appeared in the other three tests with OFG. Figure 13 shows the settlement in the evolution of suffusion in test OFG-H2. It can be found that the variation of settlement in tests with OFG is significantly different from that without OFG depicted in Fig. 9. The existence of OFG significantly increases the settlement induced by blowout; simultaneously, it makes the settlement unstable after blowout. In test OFG-H2, suffusion initiated at $\Delta H = 132.7$ cm, and slight increase in settlement was monitored at the early stage of $\Delta H = 132.7$ cm, and it increased from 2.16 mm at $\Delta H = 111.8$ cm to 2.18 mm at $\Delta H = 132.7$ cm. During the progression of suffusion, settlement kept constant when ΔH increased from 132.7 to 186.8 cm. When ΔH increased to 214.0 cm, blowout occurred, significant and sudden change in settlement was observed at the late stage of $\Delta H = 214.0$ cm, and it increased from 2.18 to 2.28 mm. What is worse, it was also found that the settlement after blowout was not stable, and it continuously increased from 2.28 mm at $\Delta H = 214.0$ cm to 2.30 mm at $\Delta H = 302.0$ cm, 2.32 mm at $\Delta H = 428.6$ cm, and 2.34 mm at $\Delta H = 550.1$ cm. The net change in settlement induced by blowout in test OFG-H2 is up to 0.16 mm, while the net change in test without OFG is only 0.06 mm. So it can be concluded that OFG in

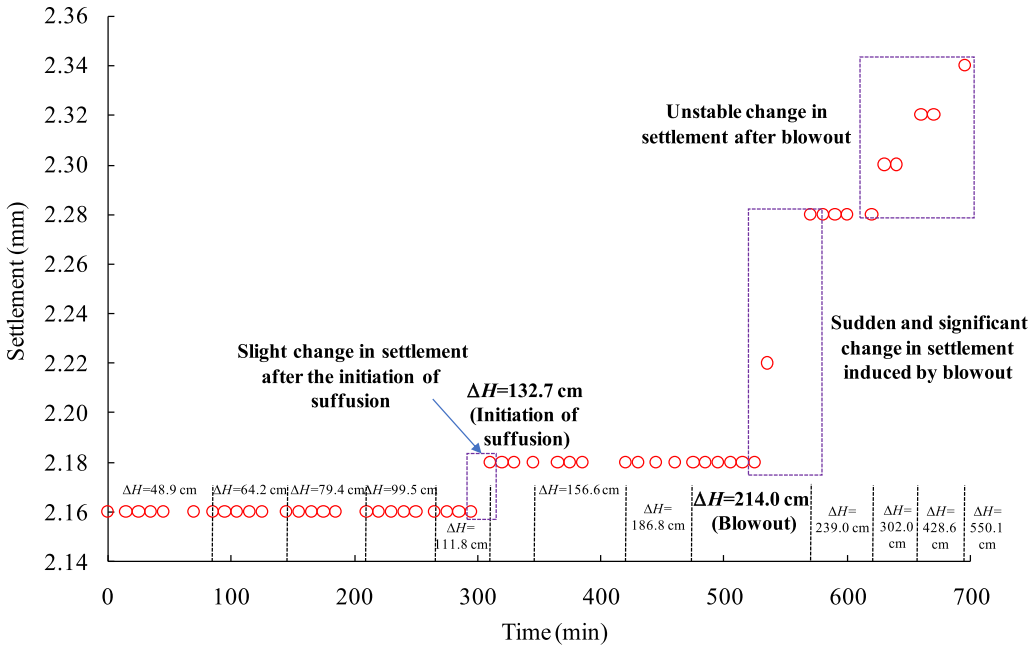

Fig. 13 Settlement in evolution of suffusion (test OFG-H2)

the field is likely to induce unacceptable deformation of foundation, and it is really a significant threat for dam safety.

3.5 Fine particles eroded into OFG after suffusion tests

After each test, the grain size distribution of OFG was determined by sieve analysis according to ASTM D6913-04 [2]. Figure 14 depicts the changes in particle size distributions of OFG after suffusion tests. It can be found that a large number of fine particles and some coarse particles finer than 2 mm in the sandy gravel adjacent to OFG were eroded into OFG. Simultaneously, the mass of the eroded particles gradually decreased with the increase in x_c. For example, the particles eroded into the OFG in test OFG-H1 consist of about 8% fine particles (according to Sect. 2.2, the division between fine and coarse particles is 0.7 mm for the sandy gravel in this study) and 1.74% coarse particles with diameters ranging from 0.7 to 2 mm.

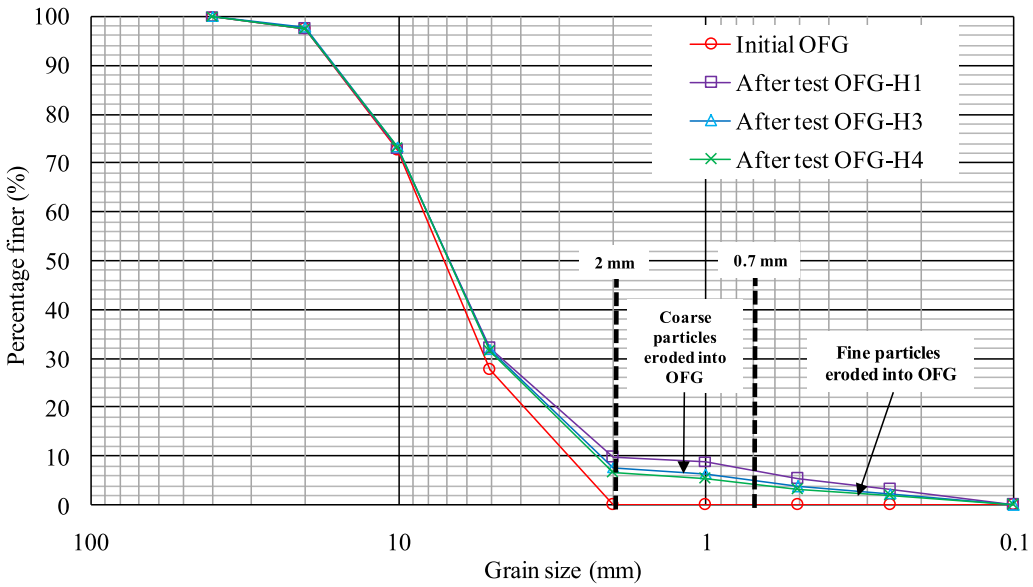

Fig. 14 Changes in particle size distributions of OFGs after suffusion tests

Similarly, in test OFG-H4, the particles eroded into OFG consist of about 4% fine particles (finer than 0.7 mm) and 2.61% coarse particles with diameters ranging from 0.7 to 2 mm.

Changes in particle size distributions of OFG after suffusion tests also explain the variation of the hydraulic gradient of OFG in the evolution of suffusion, as depicted in Fig. 11. At the early stage of test, the permeability of OFG is far greater than the surrounding sandy gravel; consequently, the hydraulic gradient of OFG is significantly low, such as $i_{21-22} = 0.06$ depicted in Fig. 11a. Once suffusion initiated, fine particles started to migrate into OFG, and then, the permeability of the OFG started to decrease gradually. After blowout, more fine particles and some coarse particles started to migrate into OFG, and then, the permeability of OFG started to decrease significantly with the increase in the fine particle content of OFG, so the hydraulic gradient of OFG at the later stage of test increased significantly, such as $i_{21-22} = 0.84$ depicted in Fig. 11d.

4 Conclusions

Five flume-scale suffusion tests were performed to investigate the influence of OFG on suffusion at the bottom of a cutoff wall in sandy gravel alluvium. The results indicate that suffusion in the tests with OFG is significantly different from that without OFG. In the test without OFG, suffusion first initiates at the downstream side of the tip of the cutoff wall, while in the tests with OFG, suffusion first initiates at the upstream side of OFG, and then both generally progress backward to the upstream side. OFG significantly decreases the hydraulic gradients at the initiation of suffusion and at blowout. In addition, a large number of fine particles and some coarse particles finer than 2 mm in the sandy gravel adjacent to OFG were observed to be eroded into OFG in the tests. Meanwhile, OFG significantly increases the settlement induced by blowout and makes the settlement unstable after blowout. So OFG is completely possible to be an internal seepage exit of fine particle migration in the field, and it is likely to change and accelerate the evolution of suffusion and finally threatens dam safety. It suggests that before cutoff wall is built, it should comprehensively check out whether there is OFG adjacent to the tip of the cutoff wall or not.

Acknowledgements The supports of National Key Research and Development Program of China under Project No. 2017YFC1502603, Natural Science Foundation of China under Project No. 51679070, Fundamental Research Funds for the Central Universities under Project No. 2018B11714, and Priority Academic Program Development of Jiangsu Higher Education Institutions are gratefully acknowledged.

References

1. ASTM (2006) Standard test method for permeability of granular soils (constant head). ASTM international. D2434-68, West Conshohocken, PA
2. ASTM (2009) Standard test methods for particle-size distribution (gradation) of soils using sieve analysis. D6913-04, West Conshohocken, PA
3. Benamar A, Correia dos Santos RN, Bennabi A, Karoui T (2019) Suffusion evaluation of coarse-graded soils from Rhine dikes. Acta Geotech 14:815–823. https://doi.org/10.1007/s11440-019-00782-1
4. Bendahmane F, Marot D, Alexis A (2008) Experimental parametric study of suffusion and backward erosion. J Geotech Geoenviron Eng 134:57–67. https://doi.org/10.1061/(ASCE)1090-0241(2008)134:1(57)
5. Chang DS, Zhang LM (2013) Critical hydraulic gradients of internal erosion under complex stress states. J Geotech Geoenviron Eng 139:1454–1467. https://doi.org/10.1061/(ASCE)GT.1943-5606.0000871
6. Chang DS, Zhang LM (2013) Extended internal stability criteria for soils under seepage. Soils Found 53:569–583. https://doi.org/10.1016/j.sandf.2013.06.008
7. Correia dos Santos RN, Caldeira LMMS, das Neves EM (2015) Experimental study on crack filling by upstream fills in dams. Géotechnique 65:218–230. https://doi.org/10.1680/geot.14.P.198
8. Correia dos Santos RN, Caldeira LMMS, das Neves EM (2014) Laboratory test for evaluating crack filling during internal erosion in zoned dams. Geotech Test J 37:463–476. https://doi.org/10.1520/gtj20130104
9. Fannin RJ, Slangen P (2014) On the distinct phenomena of suffusion and suffosion. Geotech Lett 4:289–294. https://doi.org/10.1680/geolett.14.00051
10. Fell R, Macgregor P, Stapledon D, Bell G, Foster M (2014) Geotechnical engineering of dams, 2nd edn. CRC Press, Leiden
11. Ferreira JT, Ritzi RW Jr, Dominic DF (2010) Measuring the permeability of open-framework gravel. Ground Water 48:593–597. https://doi.org/10.1111/j.1745-6584.20
12. Foster M, Fell R, Spannagle M (2000) A method for assessing the relative likelihood of failure of embankment dams by piping. Can Geotech J 37:1025–1061. https://doi.org/10.1139/cgj-37-5-1025
13. Indraratna B, Nguyen VT, Rujikiatkamjorn C (2011) Assessing the potential of internal erosion and suffusion of granular soils. J Geotech Geoenviron Eng 137:550–554. https://doi.org/10.1061/(asce)gt.1943-5606.0000447
14. Jussel P, Stauffer F, Dracos T (1994) Transport modeling in heterogeneous aquifers: 1. Statistical description and numerical generation of gravel deposits. Water Resour Res 30:1803–1817. https://doi.org/10.1029/94wr00162
15. Kenney TC, Lau D (1985) Internal stability of granular filters. Can Geotech J 22:215–225. https://doi.org/10.1139/t86-068
16. Ke L, Takahashi A (2014) Experimental investigations on suffusion characteristics and its mechanical consequences on saturated cohesionless soil. Soils Found 54:713–730. https://doi.org/10.1016/j.sandf.2014.06.024
17. Li M, Fannin RJ (2008) Comparison of two criteria for internal stability of granular soil. Can Geotech J 45:1303–1309. https://doi.org/10.1139/T08-046
18. Li M, Fannin RJ (2012) A theoretical envelope for internal instability of cohesionless soil. Géotechnique 62:77–80. https://doi.org/10.1680/geot.10.T.019
19. Lunt IA, Bridge JS (2007) Formation and preservation of open-framework gravel strata in unidirectional flows. Sedimentology 54:71–78. https://doi.org/10.1111/j.1365-091.2006.00829.x

20. Lunt IA, Bridge JS, Tye RS (2004) A quantitative, three dimensional depositional model of gravelly braided rivers. Sedimentology 51:377–414. https://doi.org/10.1111/j.1365-3091.004.00627.x
21. Luo YL, Luo B, Xiao M (2019) Effect of deviator stress on the initiation of suffusion. Acta Geotech. https://doi.org/10.1007/s11440-019-00859-x
22. Luo YL, Nie M, Xiao M (2017) Flume-scale experiments on suffusion at the bottom of cutoff wall in sandy gravel alluvium. Can Geotech J 54:1716–1727. https://doi.org/10.1139/cgj-2016-0248
23. Marot D, Rochim A, Nguyen HH, Bendahmane F, Sibille L (2016) Assessing the susceptibility of gap-graded soils to internal erosion: proposition of a new experimental methodology. Nat Hazards 83:365–388. https://doi.org/10.1007/s11069-016-2319-8
24. Moffat RM, Fannin RJ, Garner SJ (2011) Spatial and temporal progression of internal erosion in cohesionless soil. Can Geotech J 48:399–412. https://doi.org/10.1139/T10-071
25. Moffat RM, Fannin RJ (2011) A hydromechanical relation governing the internal stability of cohesionless soil. Can Geotech J 48:413–424. https://doi.org/10.1139/T10-070
26. Ramanathan R, Guin A, Ritzi RW Jr et al (2010) Simulating the heterogeneity in braided channel belt deposits: part 1. A geometric-based methodology and code. Water Resour Res 46:475–478. https://doi.org/10.1029/2009WR008111
27. Rice JD, Duncan JM (2010) Findings of case histories on the long-term performance of seepage barriers in dams. J Geotech Geoenviron Eng 136:2–15. https://doi.org/10.1061/(ASCE)GT.1943-5606.0000175
28. Sibille L, Marot D, Sail Y (2015) A description of internal erosion by suffusion and induced settlements on cohesionless granular matter. Acta Geotech 10:735–748. https://doi.org/10.1007/s11440-015-0388-6
29. Skempton AW, Brogan JM (1994) Experiments on piping in sandy gravels. Géotechnique 44:449–460. https://doi.org/10.1680/geot.1994.44.3.449
30. Terzaghi K (1925) Erdbaumechanik. Deuticke, Vienna
31. Ul Haq I (1996) Tarbela Dam: resolution of seepage. Proc Inst Civ Eng Geotech Eng 119:49–56. https://doi.org/10.1680/igeng.1996.28135
32. Wan CF, Fell R (2004) Experimental investigation of internal instability of soils in embankment dams and their foundations. UNICIV report R429, the University of New South Wales, Sydney, Australia
33. Wan CF, Fell R (2008) Assessing the potential of internal instability and suffusion in embankment dams and their foundations. J Geotech Geoenviron Eng 134:401–407. https://doi.org/10.1061/(ASCE)1090-0241(2008)134:3(401)